Lift Losses for Fin-Body Gaps in Transonic and Supersonic Speeds

Ameer G. Mikhail*
U.S. Army Ballistic Research Laboratory, Laboratory Command
Aberdeen Proving Ground, Maryland 21005

An algebraic model is established to predict the fin-lift losses due to fin-body gaps for missiles and projectiles in transonic and supersonic speeds. The model is based on two distinct correlations, which were established based on wind-tunnel results. The first correlation and model is for transonic speeds ($0.8 \le M \le 1.2$) for large fin-gap heights ($g/D \ge 0.08$) to complete the earlier work of Mikhail ("Fin Gaps and Body Slots: Effects and Modeling for Guided Projectiles," AIAA Paper 87-0447, Jan. 1985), which was only valid for ($g/D < 0.08$). The second correlation and model is for both small and large gaps at supersonic speeds ($1.2 < M < 4$). Both correlations use the physical parameters of the fin as well as the flow conditions. The results obtained using these two correlations are very satisfactory when compared with the data that they represent. There is no alternate approach in the literature that can predict these results. The correlations cover all shapes of fin planforms with moderate aspect ratios (0.5–4.0) and all heights of streamwise gaps. The present model includes viscosity and fin-support interference effects based on actual wind-tunnel measurements, which, of course, encompass both effects. The present analysis utilizes very simple algebraic models, which can be easily implemented in any fast aerodynamic prediction code. Eighteen cases were validated against experiments using the present two models.

Nomenclature

A, A_1, A_2 = fin total surface area, one side only
$A_{10}, A_{11}, A_{20}, A_{22}$ = fin partial surface area, one side only
AR = fin aspect ratio, $(2b)^2/s$
A_f = fin surface area, one side only of one fin panel
AF = fin area correlation factor
A_g = streamwise gap area for one fin panel
b = fin semispan, without a gap
b_1, b_2 = a prescribed fin height, without a gap
BF = boundary-layer correlation factor
c, c_1, c_2 = fin-root chord length
CF = overall fin correlation factor
C_N = normal force coefficient, based on the body reference area, = normal force/qs_{ref}
C_{N_f} = fin (and its interference) normal force coefficient based on the body reference area
$C_{N_{fg}}$ = fin (and its interference) normal force coefficient in presence of a fin gap g
C_{N_α} = normal force slope coefficient, per radian
$C_{N_{\alpha f}}$ = fin (and its interference) normal force slope coefficient, per radian
$C_{N_{\alpha fg}}$ = fin (and the interference) normal forces slope coefficient, in presence of a fin gap g, per radian
CSF = fin-chord and -span correlation factor
D = body diameter
FNF = fin normal force loss factor, due to presence of a fin gap g
g, g_1, g_2 = gap height between fin root chord and body surface
GF = fin-gap correlation factor
M = Mach number of projectile
q = dynamic pressure of the flow, $0.5\rho_\infty U_\infty^2$
R_e, R_{e1}, R_{e2} = Reynolds number of the projectile per unit length $\rho_\infty U_\infty/\mu_\infty$
R_{e_x} = local Reynolds number of the projectile flow, $\rho_\infty U_\infty x/\mu_\infty$
S = fin surface area (one side) of two fin panels connected without gaps and body diameter
S_{ref} = body reference area, $\pi D^2/4$
SF = fin shape correlation factor
x = distance along the body axis from the nosetip
x_{LE}, x_{LE1}, x_{LE2} = distance along the body axis from the nosetip to the leading edge of a fin panel at the fin-root section
α = angle of attack
δ = boundary-layer thickness
$\delta_{LE}, \delta_{LE1}, \delta_{LE2}$ = boundary-layer thickness at the leading edge of the fin-root section

Subscript
g = indicates the presence of a gap between fin root chord and body surface

I. Introduction

THERE has been an increasing interest by the Army in "smart munitions." Smart munitions are those guided to their targets by laser, millimeter wave, radar, or any other means. They require in-flight controllability, which is usually achieved by rotatable control surfaces (fins/tails/wings/canards). These surfaces usually require some small gaps or "clearances" with the body of the projectile as depicted in Fig. 1. These "small" gaps always result in loss of lift produced by the fins. These losses were studied in detail by Mikhail[1] for the transonic speed regime ($M = 0.8 - 1.2$) and small gaps ($g/D < 0.08$ where D is the body diameter). The specific range of interest of Ref. 1 was dictated by the Copperhead guided-projectile case study. Mikhail's correlation[1] is not applicable in the supersonic speed regime ($M = 1.2 - 4$) or for large gaps ($g/D > 0.08$).

Large gap heights, defined in this study as those with $g > 0.08\ D$, are used for reasons other than body clearance. For maneuverability of guided missiles and projectiles, the vehicle must be less statically stable so that the required control sur-

Presented as Paper 89-0332 at the AIAA 27th Aerospace Sciences Meeting, Reno, NV, Jan. 9-12, 1989; received March 7, 1989; revision received Jan. 2, 1990.

*Aerospace Engineer, Launch and Flight Division. Senior Member AIAA.

face can be small and yet sufficient to "steer" the vehicle into its desired path. To reduce static stability in the guided phase of the vehicle, a fin-body gap may be created by actuators that push the fins away from the body. These gaps are usually larger than those required only to clear the body to allow the motion of the fin.

The present study covers the Mach number and gap height ranges which were not covered in Ref. 1. Figure 2 shows the small range of applicability of Ref. 1, as given by region I, whereas the present study covers regions II and III.

The present work uses the data of Ref. 2, which provides data for missiles with and without gaps for the present ranges of study. References 3–5 provide additional experimental data. However, unlike their use in Ref. 1, these data cannot be used in this study. Their Mach range and gap heights were covered and used for the range of interest of Ref. 1.

Some earlier analytic work was done, primarily for supersonic speeds. This work usually neglects viscosity effects, which are very dominant for the small gaps, and also neglects the fin-body support effects. The present analysis avoids these two difficult-to-predict phenomena by utilizing measured data where these effects are both included. Bleviss and Struble[6] in 1953 presented an inviscid analysis of gap losses for triangular fins in supersonic speeds. The analysis is only valid for triangular fins and neglects viscosity effects. It also assumes a long afterbody extending beyond the fin location. Mirles,[7] almost at the same time, presented a slender-body analytic solution for the fin-lift losses for the same limitation of triangular fin, long afterbody behind the fins, no viscosity and no fin support interference. Dugan and Hikido,[8] shortly after in 1954, presented a slender-body analysis for gap effects for triangular fins mounted on long afterbodies with no viscosity or fin support interference effects considered. A more recent analytic work was done by August[9] in 1982, who used the inviscid supersonic analysis of Bleviss and Struble and the ambiguous results of Hoerner[10] at subsonic speeds to estimate the normal force losses for streamwise gaps. The application was made to the typical triangular fin of aspect ratio 1.0. August applied the analysis to the Sidewinder missile geometry at $M = 2.5$ for the triangular canard fin with fin deflection. The gap area was estimated and equalized by a streamwise gap area. This application was done during the development of a fast aerodynamic design code. Suh et al.,[11] in 1984, reiterated the results of August and made an application to a missile configuration at $M = 1.2$ and 2.0 using the same computer code. In both cases of Refs. 9 and 11, no details of the geometry and test conditions were given nor was a systematic calculation procedure stating the limitations and restrictions disclosed.

It is the purpose of this paper to systematically account for the lift (or normal force at zero angle of attack) loss due to streamwise fin-body gaps for large and small gaps in both the transonic and supersonic speed regimes. This work complements the earlier work of Ref. 1 and completes the coverage of the fin loss for all speed regimes and gap heights of practical interest.

II. Analysis

Two distinct areas of analysis are performed. The first is for large gaps ($g/D \geq 0.08$) in transonic speeds. The second is for supersonic speeds ($1.2 < M < 4$) and for any size gap (both small and large).

For body-tail combination, one can model the effects of gaps by writing[1] the normal force coefficient of a body-tail combination $C_{N_{BT}}$ in terms of the body alone C_{N_B} and the tail alone C_{N_T} components as:

$$C_{N_{BT}} = C_{N_B} + FNF \cdot (K_{T(B)} + (K_{B(T)}) \cdot C_{N_T} \tag{1}$$

where the FNF is the fin normal force correction factor ($0 < FNF \leq 1$) and defined as for small α:

$$FNF = \frac{C_{N_{fg}}}{C_{N_f}} = \frac{C_{N_{\alpha fg}}}{C_{N_{\alpha f}}} \tag{2}$$

where $C_{N_{fg}}$ is the normal force coefficient of the fin in the presence of a gap height g.

The gap effect for an unknown case FNF_2, was correlated to the value of a known case FNF_1 by the relation

$$FNF_2 = CF \cdot FNF_1 \tag{3}$$

where CF is the correlation factor which is written as:

$$CF = (SF \cdot AF \cdot GF \cdot CSF \cdot BF) \tag{4}$$

where SF, AF, GF, CSF, and BF are the shape, fin area, gap, chord/span, and boundary-layer factors, respectively.

A. Large Gaps ($g/D > 0.08$) in Transonic Speeds ($M = 0.8 - 1.2$)

This analysis modifies the expressions of Ref. 1, which is only valid for small gaps ($g/D < 0.08$). For large gaps, it was found that modifications to only the shape, gap, and chord/span factors are needed. The new forms for these factors are as follows:

$$SF = \left\{ \frac{\left[\left(\frac{0.76A_{20}+A_{22}}{A_{22}}\right) + \frac{0.24A_{20}(A_{22}-A_{11})}{(0.5b_2c_2)(0.5b_2c_2-0.5b_1c_1)}\right]}{\left[\left(\frac{0.76A_{10}+A_{11}}{A_{11}}\right) + \frac{0.24A_{10}(A_{22}-A_{11})}{(0.5b_1c_1)(0.5b_2c_2-0.5b_1c_1)}\right]} \right\}^{0.85} \quad \text{for } (g/D)_2 > 0.08 \tag{5a}$$

$$GF = \left(\frac{(g/D)_1}{(g/D)_2}\right)^{0.2} \tag{5b}$$

$$CSF = \sqrt{\left(\frac{b_2}{b_1}\right)\left(\frac{c_2}{c_1}\right)^{1.5}} \tag{5c}$$

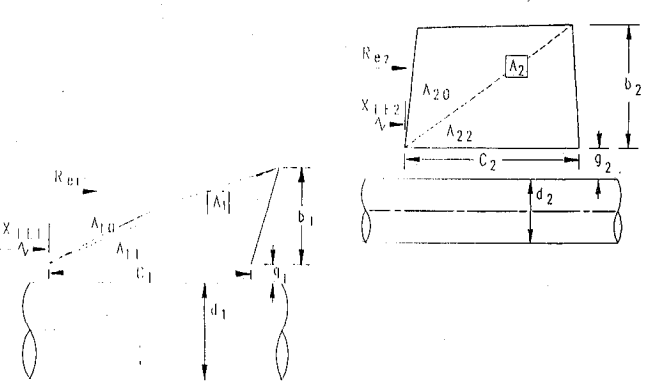

Fig. 1 Nomenclature for the fin-gap analysis.

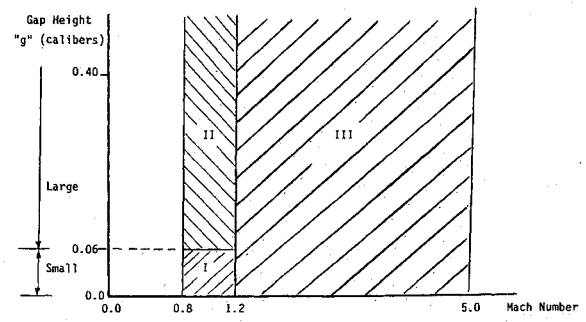

Fig. 2 Present range of application (region II and III) in comparison with the range of Ref. 1 (range 1).

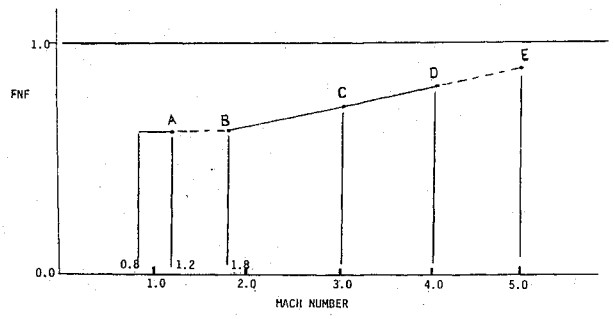

Fig. 3 The gap height factor *GF* for transonic speeds and large gaps.

where each fin area A_2 is split into one triangular area A_{22} (with its base being the fin root chord) and A_{20} for the remainder area of the fin.

The remaining two factors, *AF* and *BF*, are unchanged and are given by the expressions[1]

$$AF = \frac{A_1}{A_2} \tag{5d}$$

and

$$BF = \left(\frac{\delta_{LE2}}{\delta_{LE1}}\right)^{.88} \tag{5e}$$

where the boundary-layer thickness δ_{LE} was estimated by the familiar form[12] for turbulent boundary layers in axisymmetric tubes

$$\delta_{LE1} = 0.37 \frac{X_{LE1}}{(Re_{XLE1})^{0.2}}$$

The reference case for FNF_1 is the triangular fin of aspect ratio 1.5 of Ref. 2 with $(g/D)_1 = 0.06$, $b_1 = 0.525$ in., $c_1 = 1.4$ in., $A_{11} = 0.3675$ (in.)^2, $A_{20} = 0.3675$ (in.)^2, and $FNF_1 = 0.795$.

One would notice that the three new expressions [Eqs. (5a–5c)] represent simple modifications to the original expressions of the small gaps. The power of 0.85 was used instead of 1.0 for the shape factor *SF*. The *GF* factor power was simplified to 0.2 instead of the earlier form

$$\frac{1}{\left[1.6 - \left(\frac{(g/D)_1}{(g/D)_2}\right) \cdot \left(\frac{(g/D)_2 - 0.04}{0.05}\right)\right]}$$

Finally, the power 1.5 was used in the *CSF* factor [Eq. (5c)] instead of 1.0.

The new *GF* function for large gaps differs significantly in value compared to the corresponding *GF* function of Ref. 1 for small gaps. The two functions are plotted in Fig. 3. This large gap model must be used for $g/D \geq 0.08$, whereas the small gap model must be used for $g/D < 0.06$. For $0.06 < g/D < 0.08$, either function may be used but only with its associate formulas.

One should notice the absence of Mach number dependency, a fact which was established in Ref. 1 for the transonic speed regime ($M = 0.8 - 1.2$). This observation will not be true for the supersonic speed regime, as will be shown next.

B. Large and Small Gaps in Supersonic Speeds ($M = 1.2 - 4.0$)

It was found, by examining the data of Ref. 2, that Mach number independence of *FNF* can be extended to $M = 1.8$ as indicated in Fig. 4. The data also showed linear behavior in the Mach range 1.8–4.0. Therefore, if the value of *FNF* is predicted at $M = 4.0$ (point *D*), then the *FNF* can be easily computed over the supersonic region between $M = 1.2$ and 4.0. The decrease in the lift loss with increasing Mach number may be due to the thining of the boundary layer thickness crossing the gap.

The data available at Mach 4.0 in Ref. 2 were less in number than those available from the same reference for $M = 3.0$ (point *C*). Therefore, the correlation was based on the data at $M = 3.0$, and the model then linearly extends the value to $M = 5.0$ as shown also in Fig. 4. The value of *FNF* at $M = 1.8$ (point *B*) is already known for small gaps (Ref. 1) and for large gaps (from the preceding section).

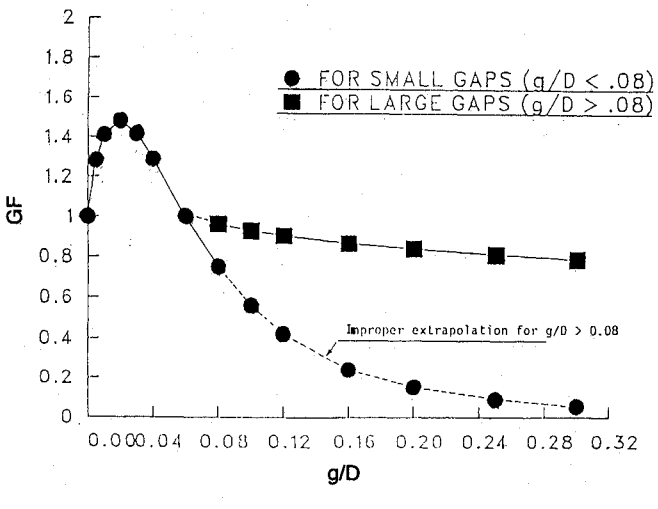

Fig. 4 The model for fin normal force losses in supersonic speeds.

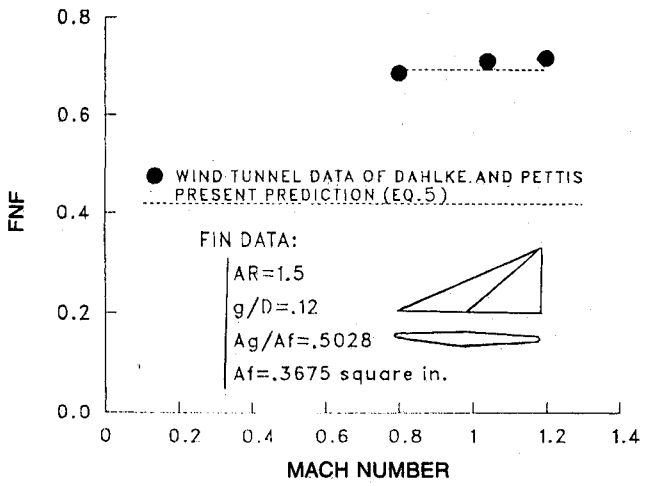

Fig. 5 Comparison with data, transonic speeds ($AR = 1.5$, $g/D = 0.12$).

The *FNF* model at Mach 3.0 was constructed in a similar manner as that of Ref. 1, however, with some parameters being changed. First, the shape factor was not influential and the Reynolds number dependency was very weak. The wind-tunnel data correlated better using the aspect-ratio parameter, AR, rather than the previously used area factor. Also, the chord/span parameter showed direct dependency only on the chord c. The fin span-parameter was absorbed (implicitly) in the aspect-ratio parameter.

Finally, the FNF_2 at Mach 3.0 was obtained as:

$$FNF_2|_{M=3} = CF \cdot FNF_1|_{M=3}$$

$$= \left[\left(\frac{(g/D)_1}{(g/D)_2}\right)^{.15}\left(\frac{AR_2}{AR_1}\right)^{.2}\left(\frac{c_1}{c_2}\right)^{.4}\right] \cdot FNF_1|_{M=3} \qquad (6)$$

The reference case values (case denoted by subscript 1) are the values for the case of the triangular fin of Ref. 2 at $M = 3$ with the following parameters:

$$(g/D)_1 = 0.06,\ AR_1 = 1.5,\ c_1 = 1.4 \text{ in.}$$

$$b_1 = 0.525 \text{ in. and } FNF_1|_{M=3} = 0.851 \qquad (7)$$

With the given geometric parameters of the given fin (2) $[(g/D)_2, AR_2$, and $c_2]$, one can directly calculate $FNF_2|_{M=3}$. Then, for any value of Mach number, the linear model of Fig. 4 is used to determine the corresponding FNF_2 value. Equation (1) can then be used to calculate the effective normal force for the body-tail combination with the specified gap height.

III. Results

The results provided here are for the configurations and test conditions of Ref. 2. The fin geometries and the wind-tunnel conditions were also stated in Ref. 1.

A. Large Gaps, Transonic Speeds (M = 0.8–1.2)

All cases of Ref. 2 were studied. Six cases with large-gap heights of $0.12D$, $0.16D$, $0.20D$, and $0.25D$ for fins with aspect ratios of 0.5, 0.75, 1.0, and 1.5 were computed.

Figure 5 shows the results for the *FNF* loss factor for the triangular fin of $AR = 1.5$ and a large gap height of $0.12D$. The result of the expression of Eq. (5) fits the data very well. The fin effectiveness factor computed (*FNF*) was 0.69, thus indicating a 31% loss in lift due to the gap.

Figure 6 shows the results for the same fin – but at the larger gap height of $0.20D$. The agreement is excellent between the data and the fit provided by the given correlation. A 38% lift loss is observed.

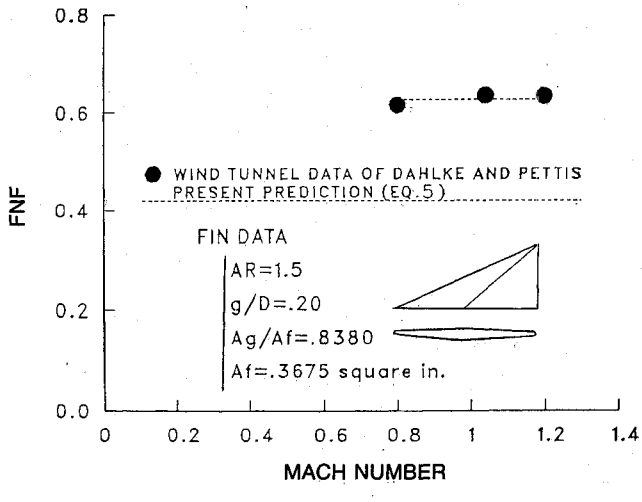

Fig. 6 Comparison with data, transonic speeds ($AR = 1.5$, $g/D = 0.20$).

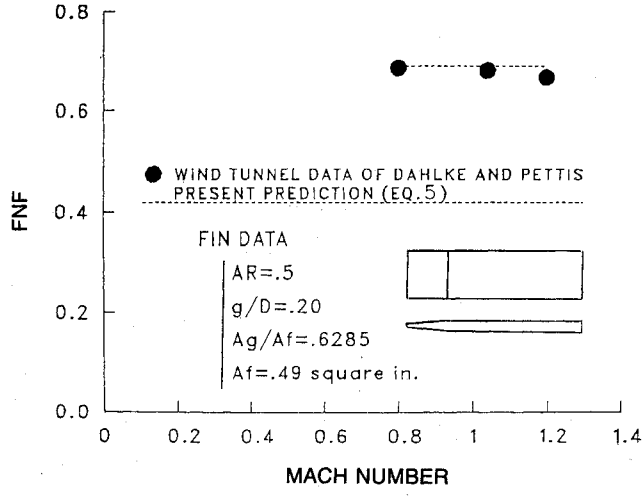

Fig. 8 Comparison with data, transonic speeds ($AR = 0.5$, $g/D = 0.20$).

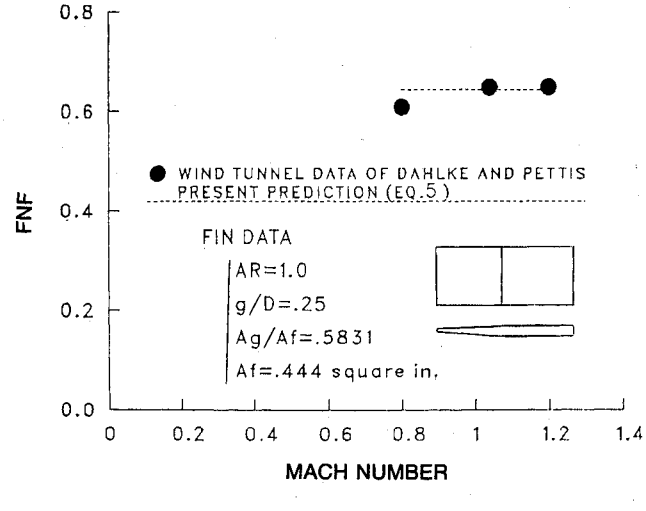

Fig. 7 Comparison with data, transonic speeds ($AR = 1.0$, $g/D = 0.25$).

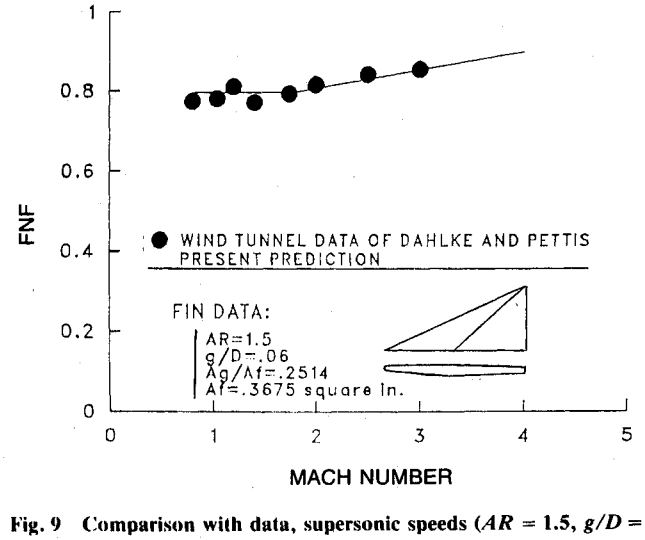

Fig. 9 Comparison with data, supersonic speeds ($AR = 1.5$, $g/D = 0.06$).

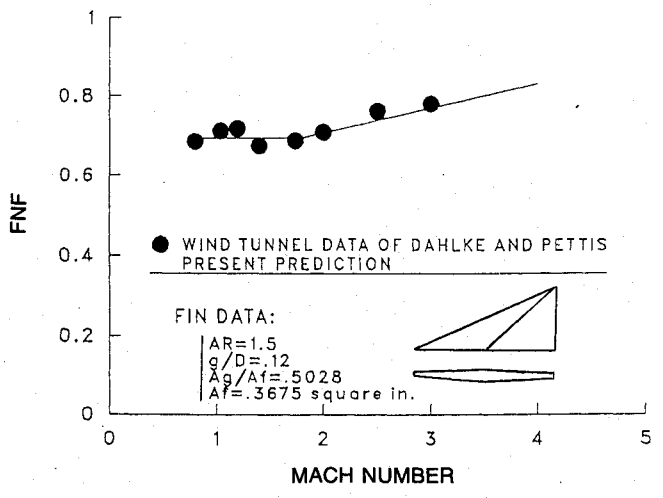

Fig. 10 Comparison with data, supersonic speeds ($AR = 1.5$, $g/D = 0.12$).

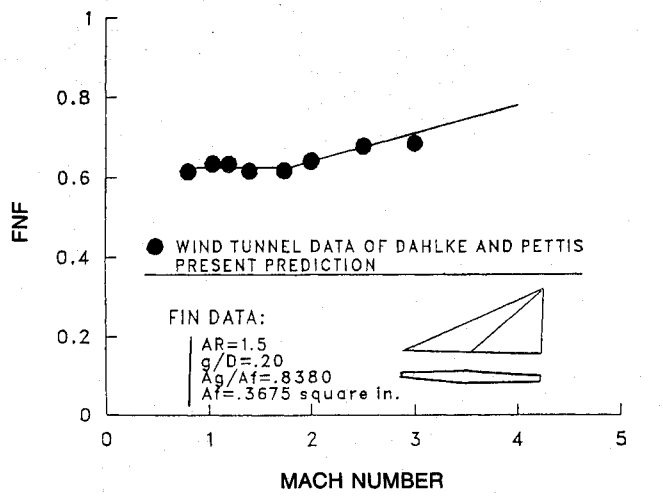

Fig. 11 Comparison with data, supersonic speeds ($AR = 1.5$, $g/D = 0.20$).

Figure 7 shows the results for a rectangular fin with an aspect ratio of 1 and gap height of $0.25D$. The fin effectiveness is 0.64, indicating a corresponding lift loss of 36%. The results agree with the data very well.

Figure 8 shows the results for a rectangular fin of $AR = 0.5$ at gap heights of $0.20D$. Even at this very small aspect ratio, the results of the established expressions are in excellent agreement with the experimental data. The fin-lift effectiveness is 0.69, indicating a corresponding lift loss of 31%, respectively.

B. Large and Small Gaps, Supersonic Speeds ($M = 1.2$–4.0)

All test cases of Ref. 2 were analyzed. Overall twelve cases were utilized; four of them are for small gaps and eight are for large gaps.

Figure 9 shows the results for a rectangular fin of $AR = 1.5$ with a small gap $D = 0.06D$. The linear model gave very good agreement with the data. Also, the extrapolation at $M = 4$ proved to be very acceptable. The results indicate a 20% lift loss for transonic speeds, a loss of 15% at $M = 3.0$, and a loss of 11% at $M = 4.0$.

Figures 10 and 11 show the results for the same fin with large gap height settings of $0.12D$ and $0.20D$, respectively. The results of the correlation expression fit the data with very good agreement.

Figures 12–14 are for a rectangular fin of $AR = 1$ at gap height settings of $0.08D$, $0.16D$, and $0.25D$. The results are very acceptable when compared with the wind-tunnel data.

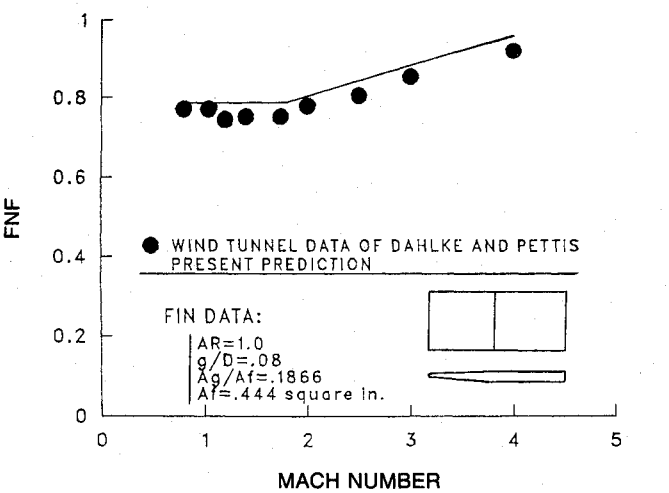

Fig. 12 Comparison with data, supersonic speeds ($AR = 1.0$, $g/D = 0.08$).

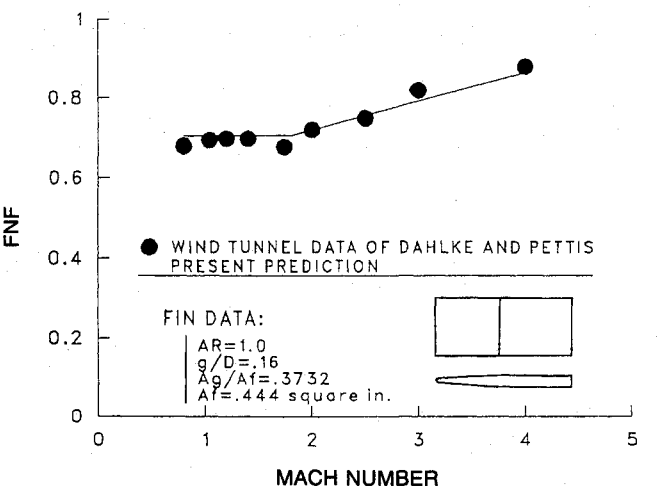

Fig. 13 Comparison with data, supersonic speeds ($AR = 1.0$, $g/D = 0.16$).

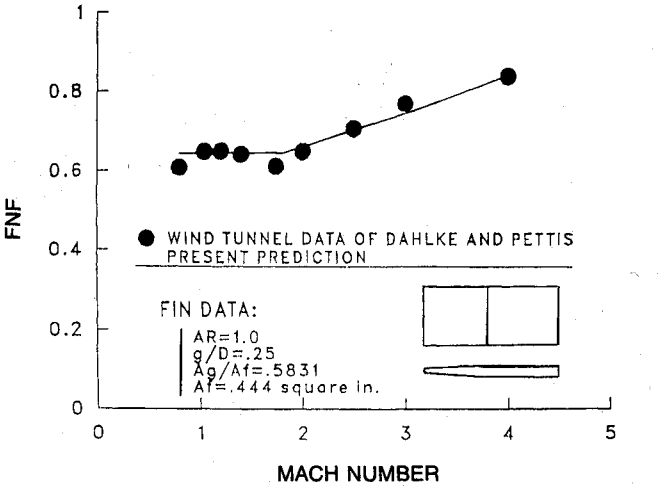

Fig. 14 Comparison with data, supersonic speeds ($AR = 1.0$, $g/D = 0.25$).

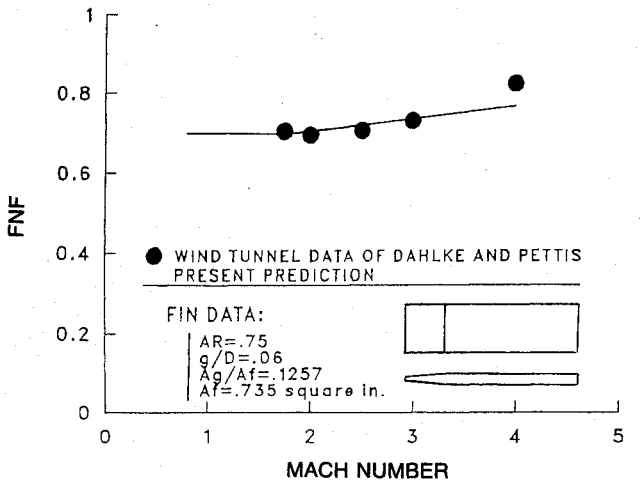

Fig. 15 Comparison with data, supersonic speeds ($AR = 0.75$, $g/D = 0.06$).

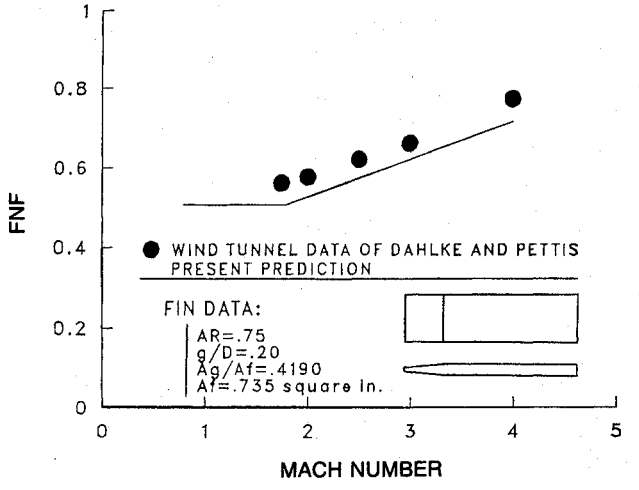

Fig. 16 Comparison with data, supersonic speeds ($AR = 0.75$, $g/D = 0.20$).

Table 1 Results of present correlations and comparison with wind-tunnel data

Case condition		*FNF* wind-tunnel data (Ref. 2)	*FNF* present correlations
I. Transonic speeds, large gaps:			
$AR = 1.5$	$g/D = 0.12$	0.709	0.692
$AR = 1.5$	$g/D = 0.20$	0.627	0.625
$AR = 1.0$	$g/D = 0.16$	0.688	0.703
$AR = 1.0$	$g/D = 0.25$	0.634	0.643
$AR = 0.5$	$g/D = 0.12$	0.766	0.764
$AR = 0.5$	$g/D = 0.20$	0.677	0.689
II. Supersonic speed, $M = 3$, large and small gaps:			
$AR = 1.5$	$g/D = 0.06$	0.851	0.851
$AR = 1.5$	$g/D = 0.12$	0.775	0.767
$AR = 1.5$	$g/D = 0.20$	0.685	0.710
$AR = 1.0$	$g/D = 0.08$	0.850	0.880
$AR = 1.0$	$g/D = 0.16$	0.816	0.791
$AR = 1.0$	$g/D = 0.25$	0.767	0.742
$AR = 0.75$	$g/D = 0.06$	0.734	0.740
$AR = 0.75$	$g/D = 0.12$	0.691	0.677
$AR = 0.75$	$g/D = 0.20$	0.659	0.619
$AR = 0.50$	$g/D = 0.06$	0.724	0.682
$AR = 0.50$	$g/D = 0.12$	0.620	0.613
$AR = 0.50$	$g/D = 0.20$	0.534	0.571

Notice the increase in the lift losses in the transonic speeds from 22 to 30 to 37% with the increase in gap height.

Figures 15 and 16 are for a rectangular fin of $AR = 0.75$ and at gap height settings of $0.06D$ and $0.20D$. The results are generally satisfactory. Note that the lift losses are 50% for the large gap of $0.20D$ in the transonic speed regime. This loss was only 30% when the gap was $0.06D$.

In general, the results appear very acceptable. For the cases considered, lift losses are predicted within 7% or less. All of the results for the 18 cases are tabulated in Table 1 together with the wind-tunnel data. The wind-tunnel Reynolds number was 0.415×10^6 per in.

IV. Summary and Conclusions

An algebraic model was established, based on wind-tunnel data correlation, that predicts the normal force losses for fins with large fin-body gaps in transonic and supersonic speeds. The present study covers a much larger range of Mach number and gap heights than those available in the present literature. The results obtained provide very good agreement with the wind-tunnel data. This work is a first in the field and provides the missile/projectile designer with a fast prediction method to calculate fin effectiveness in the presence of streamwise gaps.

The analysis covers the Mach range $0.8 < M < 4.0$ and extends the applicability to both small and large fin gap heights. The models can be used up to $M = 5.0$ with care but should not be used below $M = 0.7$. The models were validated using 18 cases of wind-tunnel tests. The model is established in simple algebraic formulas that can be easily programmed into any fast aerodynamic prediction code for missiles and projectiles. In fact, one needs only a hand calculator to obtain the results. It is a very satisfying achievement to be able to model a highly complex problem with such simple models.

References

[1]Mikhail, A. G., "Fin Gaps and Body Slots: Effects and Modeling for Guided Projectiles," AIAA Paper 87-0447, Jan. 1985; see also *Journal of Spacecraft and Rockets*, Vol. 25, No. 5, 1988, pp. 345–353.

[2]Dahlke, C. W., and Pettis, W., "Normal Force Effectiveness of Several Fin Planforms with Streamwise Gaps at Mach Numbers of 0.8 to 5.0," U.S. Army Missile Command, Redstone Arsenel, AL, Rept. RD-TR-70-8, April 1970.

[3]Killough, T. L., "Investigation of Fin Gap Effects on Static Stability Characteristics of Fin Stabilized Missile," U.S. Army Missile Command, Redstone Arsenel, AL, Rept. RF-TR-64-6, April 1964.

[4]Henderson, J. H., "An Investigation of Streamwise Body-Fin Gaps as a Means of Alleviating the Adverse Plume Effects on Missile Longitudinal Stability," U.S. Army Missile Command, Redstone Arsenel, AL, Rept. RD-77-13, Jan. 1977.

[5]Fellows, K. A., "The Effects of Gap Size on the Lift and Drag of a Simple Body with Small Rectangular Wing at Subsonic Speeds," Aircraft Research Association Limited, Bedford, England, UK, Test Code M49/15, June 1982.

[6]Bleviss, K. C., and Struble, R. A., "Some Effects of Streamwise Gaps on the Aerodynamic Characteristics of Low Aspect Ratio Lifting Surface at Supersonic Speeds," Douglas Aircraft Co., St. Louis, MO, Rept. SM-14627, April 1953.

[7]Mirles, H., "Gap Effect on Slender Wing-Body Interference," *Journal of the Aeronautical Sciences*, Vol. 20, No. 8, 1953, pp. 574–575.

[8]Dugan, W. D., and Hikido, K., "Theoretical Investigation of the Effects Upon Lift of a Gap Between Wing and Body of a Slender Wing-Body Combination," NACA TN 3224, Aug. 1954.

[9]August, H., "Improved Control Surface Effectiveness for Missiles," AIAA Paper 82-0318, Jan. 1982.

[10]Hoerner, S. F., and Borst, H. V., *Fluid Dynamic Lift*, published by the authors, 1975, Chap. 20, p. 17.

[11]Sun, J., Hansen, S. G., Cummings, R. M., and August, H., "Missile Aerodynamic Prediction (MAP) Code," AIAA Paper 84-0389, Jan. 1984; see also *Journal of Spacecraft and Rockets*, Vol. 22, No. 6, 1985, pp. 605–613.

[12]Schlichting, H., *Boundary-Layer Theory*, 6th ed., McGraw-Hill, 1968, p. 599.

Clark H. Lewis
Associate Editor